# TIME-DEPENDENT ACCRETION DISKS IN DWARF NOVAE

G.T. Bath

Dept. of Astrophysics, Oxford.

and

J.E. Pringle

Institute of Astronomy, Cambridge.

Over the past decade it has become increasingly clear that the once commonly held belief that the explosions of dwarf novae are caused by runaway thermonuclear reactions of accreted hydrogen on the surface of a white dwarf is not easily reconcilable with the growing observational data now extending from infra-red to x-ray wavelengths. It cannot fit the disk location of the outburst, the outburst energetics and repetition period (Bath et al. 1974) and the spectrum changes at outburst. The discovery that dwarf novae are semi-detached binaries opened the possibility that the explosions are caused by bursting mass accretion on to the white dwarf (Smak (1971), Bath (1973), Osaki (1974)). This model has now become a powerful tool for investigating the physical and spectroscopic properties of these systems.

We report here on a continuing programme of research on the structure of these variables, and describe a series of evolutionary models of disk changes that occur at outburst. The procedure adopted is an adaptation of the approach of Lightman (1974a, b). This generalizes stationary disk models to include time-dependence. As stressed by Lightman (1974a) and Lynden-Bell and Pringle (1974) the time-dependent structure of a viscous disk is determined by a diffusion-type equation for the surface density,

$$\frac{\partial \Sigma}{\partial t} = \frac{3}{r}\frac{\partial}{\partial r}\left\{ r^{1/2}\frac{\partial}{\partial r}\left(\mu r^{1/2}\right)\right\} \qquad (1)$$

where $\Sigma$ is the surface density and $\mu$ is the z-integrated viscosity ($= \Sigma\nu$ where $\nu$ is the effective kinematic viscosity). This diffusion equation is valid so long as the disk remains geometrically thin (sound speed, $c_s \ll$ circular velocity, $v_\phi$ ). Three other assumptions (which may be checked for consistency in the final solution) are: (1) the gravitational force is greater than the internal stress due to viscosity ($v_\phi \gg v_r$ ), (2) the radial drift timescale is greater than the radiative diffusion timescale vertically through the disk, and (3) the disk is optically thick and radiates as a black body at each radius point.



https://doi.org/10.1017/S0252921100076600 Published online by Cambridge University Press

An effective kinematic viscosity $\nu = \alpha c_s h$ is assumed, with $\alpha \leq 1$ corresponding to turbulent elements moving subsonically on scales equal to the disk height. With these assumptions time-dependence only enters the problem through the diffusion equation for $\Sigma$. All other vertically averaged variables can be derived explicitly from the surface density.

Mass transfer is introduced at time, t = 0, matter going into an orbit at radius, $r_I$, with angular momentum, $j = (GM r_I)^{\frac{1}{2}}$. Due to viscous evolution this ring spreads out toward the outer disk rim (where angular momentum is assumed to be removed efficiently through tidal interactions with the companion), and inwards toward the white dwarf surface (where mass is assumed to be accreted directly on to the surface). As the disk spreads out, the mass transfer stream collides with disk matter and circularizes. Circularization is assumed to be instantaneous. The potential energy liberated in this 'hot-spot' region is included in the energetics, but because of the assumption of cylindrical symmetry it is averaged around the entire disk rim. Effects due to the drop in opacity at $T < 10^4$ K are included.

In Fig. 1 the build-up of the disk is shown for the case in which the mass transfer rate, $\dot{m}$, is switched on at a constant value of $10^{16}$ g $s^{-1}$ at time, t = 0. The disk evolves in a typical diffusion controlled way towards the steady-state - i.e. the state for which the rate of matter input and associated addition of angular momentum exactly balances the white dwarf accretion rate and the rate of loss of angular momentum at the disk rim. The timescale on which the orbiting ring evolves into a steady disk increases as the assumed value of $\alpha$ decreases ($\alpha$ is assumed constant over all $r$ in the models described here). Models with $\alpha \sim 1$ evolve into disk structures in less than a day. Models with $\alpha \sim 10^{-6}$ take several thousand years to build up massive steady disks. Models with $\alpha \sim 10^{-12}$ take longer than the age of the Universe. The characteristic timescale for disk changes of any sort is similarly determined by $\alpha$. Values of $\alpha \sim 1$ are needed for the disk response time to be the same order ($\sim$ hours - weeks) observed in dwarf novae.

The evolution of disks with parameters typical of dwarf nova systems is presently being examined. A selection of models with a variety of functional forms for the time dependence of $\dot{m}$ are shown in Figs. 2-4. The mass transfer rate, the disk luminosity, and the evolution of disk structure ($\Sigma$ and $T_e$) are shown as functions of time. In these models $\alpha = 0.1$. It is clear that a variety of outburst morphologies are possible, depending on $\alpha$ and $\dot{m}(t)$. We find in particular that the light curve of WZ Sge is easily fitted by a sudden burst of mass accretion, followed by slow disk recovery with $\alpha \sim 0.2$. Those of dwarf novae are complicated by the strong optical 'hot-spot' contribution in the quiescent state, but dwarf nova light curves of most types are reproducible with straightforward forms for $\dot{m}(t)$.

The alternative model of the outbursts, as being caused by some ad hoc instability in the disk, has also been examined with this approach. In this case $\dot{m}$ is held constant and $\alpha$ is varied as a function of time. In Fig. 5 a case of this type is shown. In this class of model we find that strong constraints exist on the variation of $\alpha$ with time. If these are not satisfied the outbursts in no way resemble dwarf nova eruptions.



https://doi.org/10.1017/S0252921100076600 Published online by Cambridge University Press

It is not clear that these constraints can be realized with any realistic form of disk instability (if such exists). This work will be reported in detail elsewhere.

## REFERENCES


Bath, G.T. 1973, Nature Phys. Sci., 246, 84.

Bath, G.T., Evans, W.D., Papaloizou, J. and Pringle J.E. 1974, Mon.Not.R. astr.Soc., 169, 447.

Lightman, A.P. 1974a, Astrophys. J., 194, 419.

Lightman, A.P. 1974b, Astrophys. J., 194, 429.

Lynden-Bell, D. and Pringle, J.E. 1974, Mon.Not.R.astr.Soc., 168, 603.

Osaki, Y. 1974, Publ. Astron. Soc. Japan, 26, 429.

Smak, J. 1971, Asta Astronomica, 21, 15.

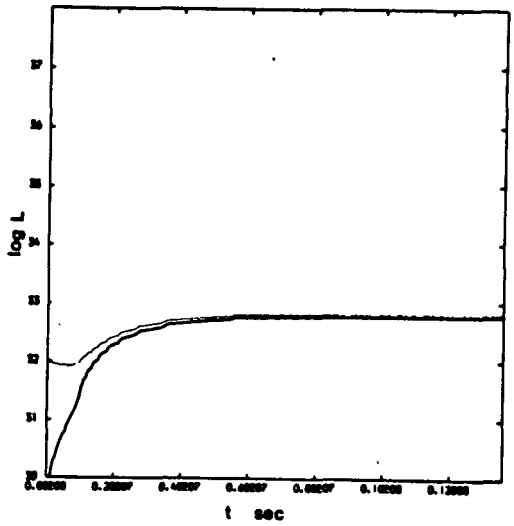


Fig. 1a.

Growth of disk luminosity, $L_{disk}$, (heavy line), and of disk and spot luminosity, $L_{disk+spot}$ (thin line) to a steady state with $\alpha = 0.1$.

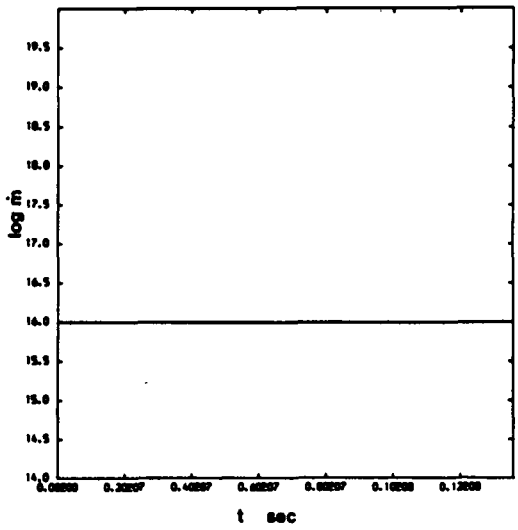


Fig. 1b.

Variation of mass transfer rate, $\dot{m}$, into disk.

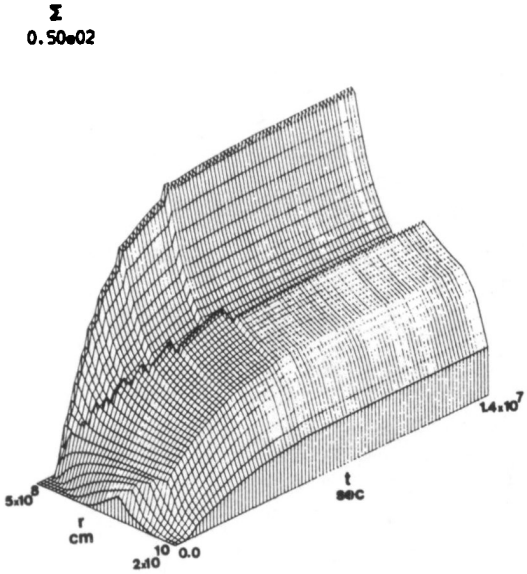


Fig. 1c.

Changes in surface density, $\Sigma$, as the disk approaches a steady-state. The maximum value of $\Sigma$ is given above (in gm $cm^2$).

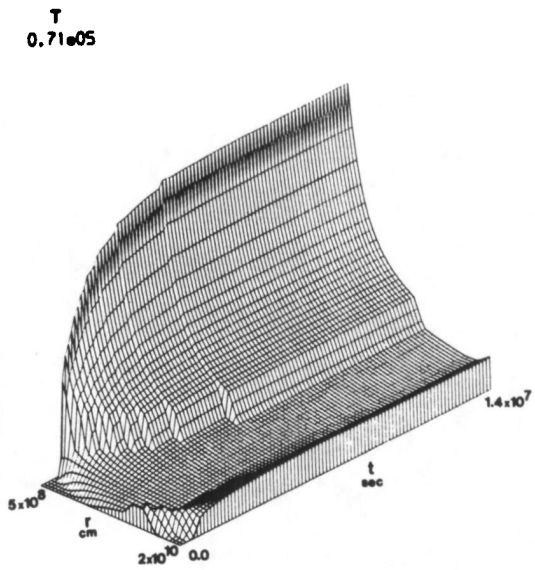


Fig. 1d.

Changes in disk temperature. The hot-spot region in the outer edge is clearly shown, together with the initial growth of the disk. At this mass transfer rate the outer disk region (apart from the spot) is cooler than $10^4$ K and probably optically thin. The maximum temperature is given above (in °K).



https://doi.org/10.1017/S0252921100076600 Published online by Cambridge University Press

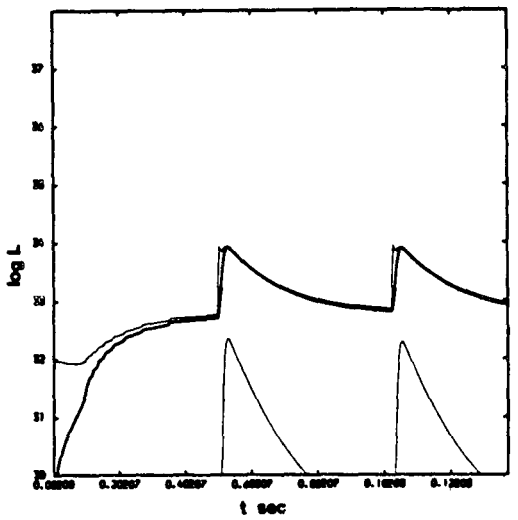


Fig. 2a.

Variation of $L_{disk}$ and $L_{disk+spot}$. The soft x-ray luminosity from the inner boundary layer (0.2-0.5 Kev) is also shown.

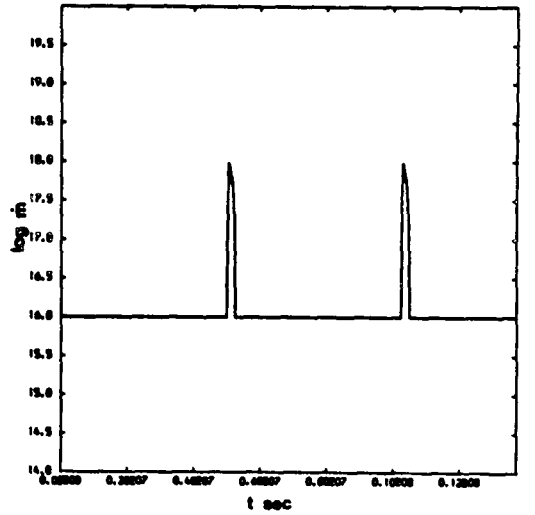


Fig. 2b.

Variation of $\dot{m}$ with time.

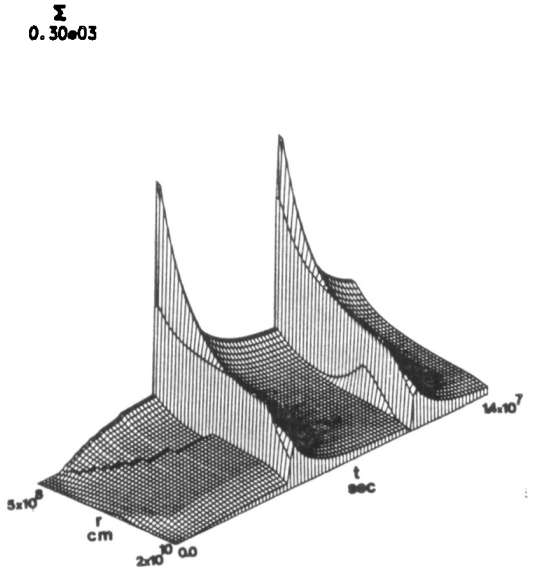


Fig. 2c.

Variation of $\Sigma$ with time. The maximum surface density is given above.

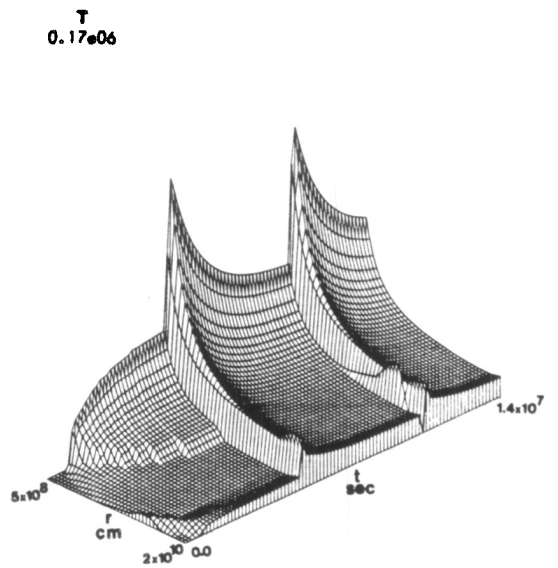


Fig. 2d.

Variation of T with time. The maximum temperature is given above.



https://doi.org/10.1017/S0252921100076600 Published online by Cambridge University Press

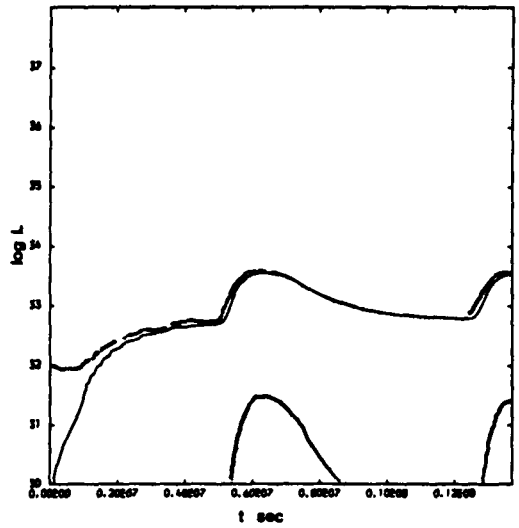


Fig. 3a.

Variation of $L_{disk}$ and $L_{disk+spot}$. The soft x-ray luminosity from the inner boundary layer (0.2-0.5 Kev) is also shown.

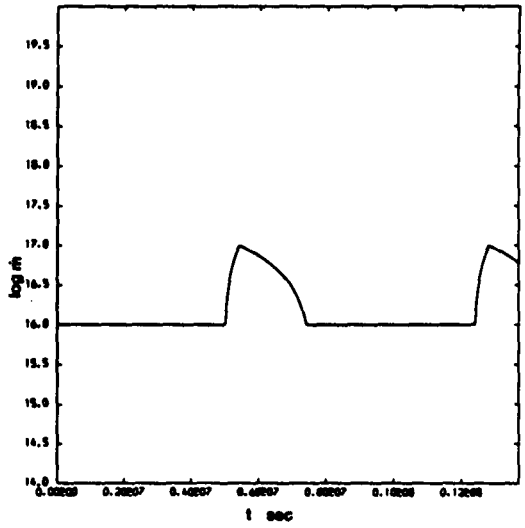


Fig. 3b.

Variation of $\dot{m}$ with time.

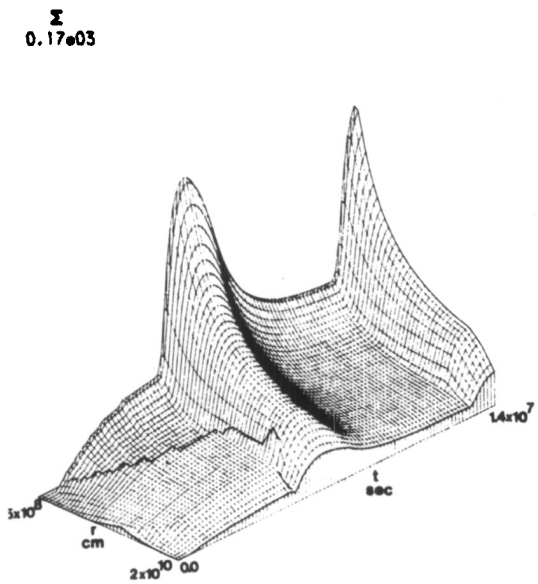


Fig. 3c.

Variation of $\Sigma$ with time. The maximum surface density is given above.

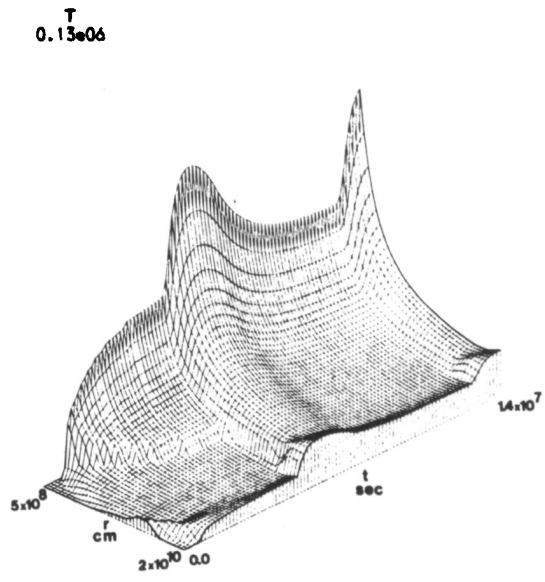


Fig. 3d.

Variation of T with time. The maximum temperature is given above.



https://doi.org/10.1017/S0252921100076600 Published online by Cambridge University Press

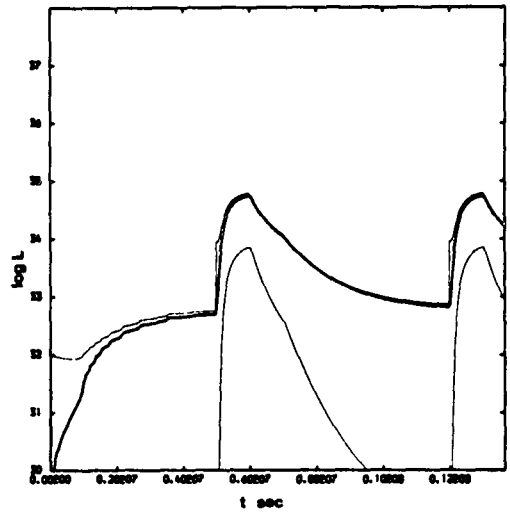


Fig. 4a.

Variation of $L_{disk}$ and $L_{disk+spot}$. The soft x-ray luminosity from the inner boundary layer (0.2-0.5 Kev) is also shown.

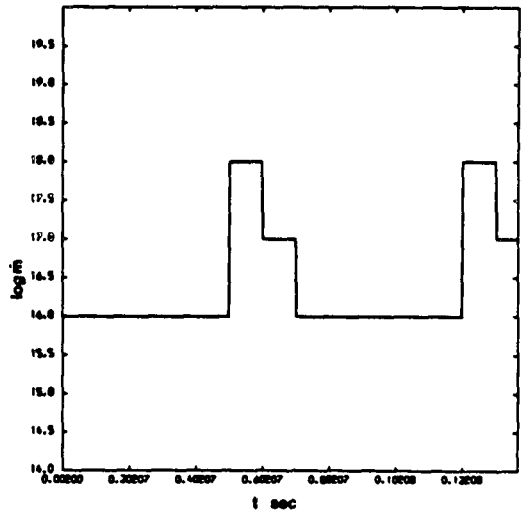


Fig. 4b.

Variation of $\dot{m}$ with time.

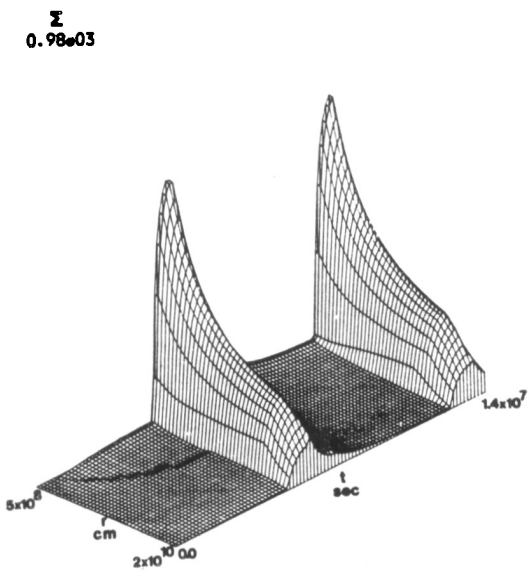


Fig. 4c.

Variation of $\Sigma$ with time. The maximum surface density is given above.

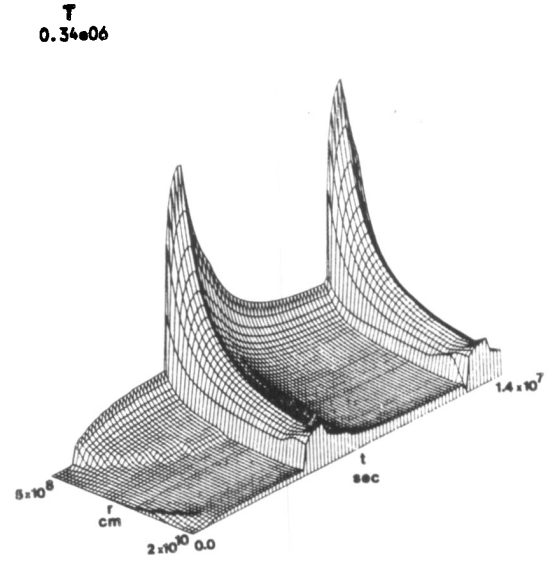


Fig. 4d

Variation of T with time. The maximum temperature is given above.



https://doi.org/10.1017/S0252921100076600 Published online by Cambridge University Press

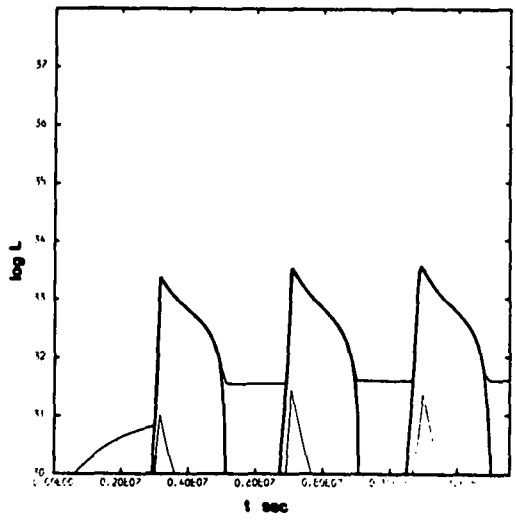


Fig. 5a.

Variation of $L_{disc}$ (thick line) and $L_{disc\ spot}$ (thin line). The soft x-ray luminosity from the inner boundary layer (0.2-0.5 Kev) is also shown.

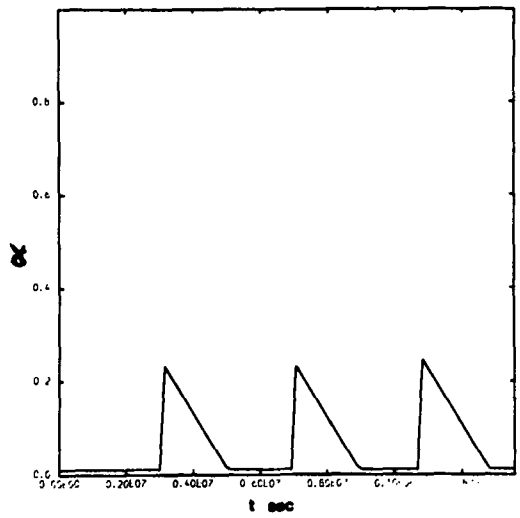


Fig. 5b.

Variation of $\alpha$ with time; $\alpha$ varies between 0.01 and 0.25 in a sawtooth pattern.

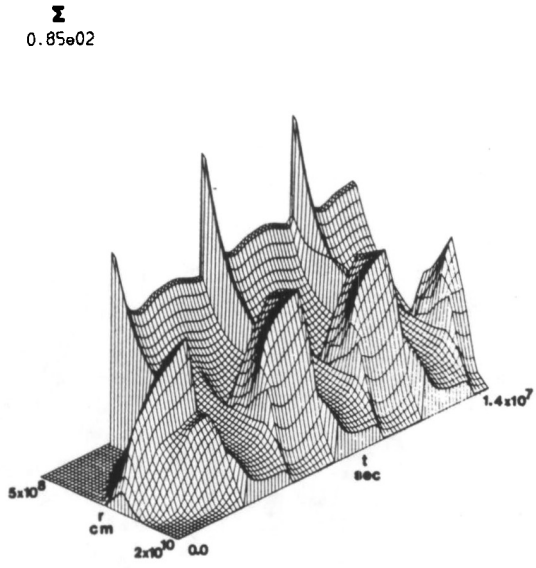


Fig. 5c.

Variation of $\Sigma$ with time. The maximum surface density is given above.

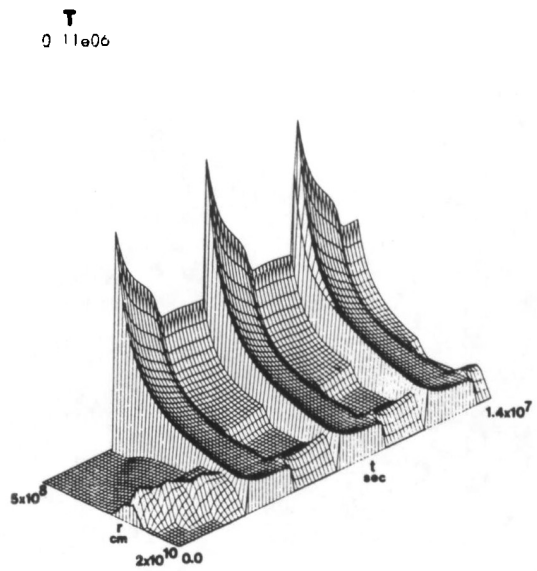


Fig. 5d.

Variation of T with time. The maximum temperature is given above.



https://doi.org/10.1017/S0252921100076600 Published online by Cambridge University Press